Microfluid Nanofluid (2015) 19:1377–1384
DOI 10.1007/s10404-015-1652-7

Magnetically controllable generation of ferrofluid droplets

Qifan Yan[1] · Shouhu Xuan[1] · Xiaohui Ruan[1] · Jie Wu[1] · Xinglong Gong[1]

Received: 13 May 2015 / Accepted: 11 September 2015 / Published online: 28 September 2015

Abstract This paper reports the manipulation of ferrofluid droplets by using a microfluidic flow-focusing device equipped with a magnetic tweezer. Besides the traditional flow rate controlling method, the magnetic field also can be applied to control the size of the droplets. Two major effects in magnetic manipulation process: magnetoviscous effect and magnetic drag effect, were studied. Under a fixed flow rate (CP = 1 mL/h, DP = 0.2 mL/h), the average sizes of ferrofluid droplets were tunable from 135 to 95 μm by varying the magnetic field from 0 to 60 mT. Moreover, square wave magnetic field can be used to periodically generate droplets with different sizes. These results are helpful to understand the generation mechanism of the ferrofluid droplet and supply a novel method for manipulating droplets with a predetermined size and distribution.

Keywords Microfluidic · Magnetic · Ferrofluid · Flow-focusing · Droplets

1 Introduction

Manipulation of small volumes liquid is important in miniaturized biological and chemical analysis, since less sample means faster reaction and lower cost. In this case, droplet-based microfluidics were developed to create discrete volume based on immiscible phases (Huebner et al. 2008; Song et al. 2006; Teh et al. 2008). In contrast to continuous flow, droplets can be individually transported, mixed and analyzed (Fair 2007; Link et al. 2006). Droplet microfluidic has the ability to process a mass of reactions at the same time without increasing device complexity. With the benefit of droplet microfluidics, large number of applications in the area of biochemical and material science like synthesis of polymer particles (Jeong et al. 2005; Nie et al. 2006), drug delivery (Ruuge and Rusetski 1993) and diagnostic testing (El-Ali et al. 2006) were realized. Therefore, controllable droplet generation and manipulation are important research topics.

There are two basic styles, passive and active, for generating the droplet. Passive methods generate and manipulate the droplets by varying the microchannel structures such as T-junction (Nisisako et al. 2002; Priest et al. 2006; Thorsen et al. 2001; Xu et al. 2006) and flow-focusing (Anna et al. 2003; Tan et al. 2006; Woodward et al. 2007; Yobas et al. 2006). Although this method has the advantage of easy fabrication, it lacks flexibility due to fixed microchannel configurations. Active methods usually combine channel structure with external sources. Electric (Abdelgawad and Wheeler 2009; Jebrail et al. 2012; Srinivasan et al. 2004; Velev et al. 2003), magnetic (Nguyen 2011; Pipper et al. 2007; Zhang et al. 2009), acoustic (Schmid and Franke 2013), optical (Diguet et al. 2009) and temperature fields (Baroud et al. 2007; Nguyen et al. 2007) are most frequently used. For the active methods, the fabrication of chip is rather complex and several bulky equipments are usually needed. To this end, an ideal droplet manipulation method should be simple in fabrication and easy in control. Among the mentioned active methods, magnetic

Electronic supplementary material The online version of this article (doi:10.1007/s10404-015-1652-7) contains supplementary material, which is available to authorized users.

✉ Xinglong Gong
gongxl@ustc.edu.cn

[1] CAS Key Laboratory of Mechanical Behavior and Design of Materials, Department of Modern Mechanics, University of Science and Technology of China, Hefei 230027, People's Republic of China

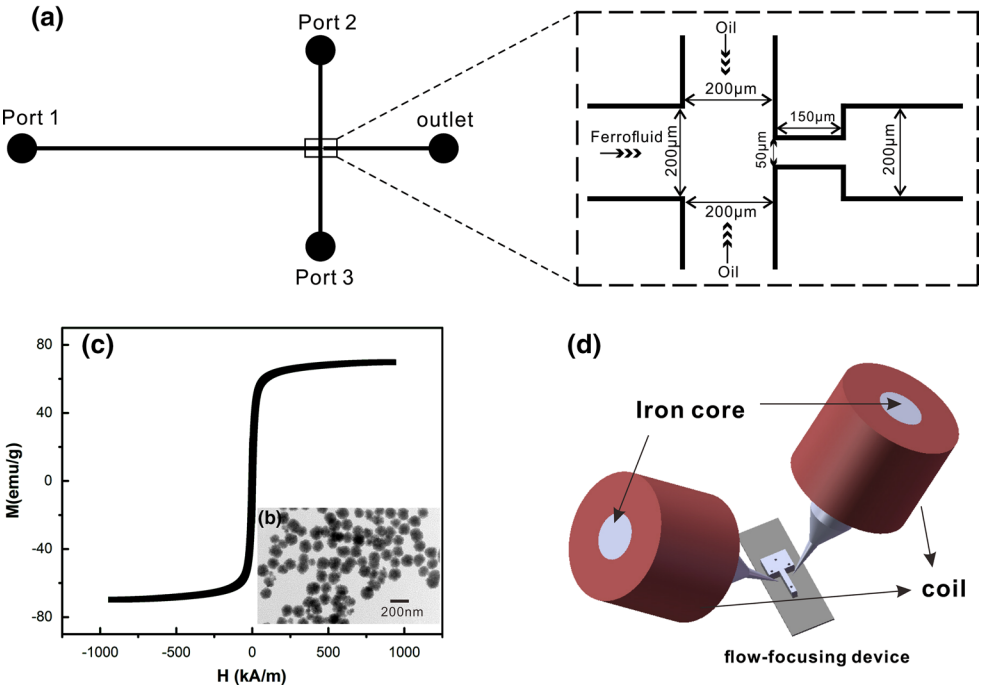

Fig. 1 **a** Schematic of the microfluidic device. Ferrofluid droplets are formed in a microfluidic flow-focusing junction. **b** TEM image and **c** magnetization curve of Fe_3O_4 nanoparticles. **d** Local field applied by magnetic tweezer device

manipulation technique has the advantage of easy realization. It could not be affected by experimental environment like pH, ionic or surface charge. With these benefits, this method was favorable.

Ferrofluids are most commonly used magnetic droplet phase. Several works were devoted to the formation mechanism of ferrofluid droplets. Tan et al. (2010) firstly reported the influence of magnet position in microfluidic T-junction. When the magnet was placed upstream, droplet size increased with increasing the magnetic flux density. In contrast, when magnet was placed downstream, droplet size decreased (Tan et al. 2010). Role of homogeneous magnetic field was also studied (Tan and Nguyen 2011; Wu et al. 2013). Both radial and axial magnetic fields can actively control the formation of ferrodroplets in flow-focusing configuration. In general, the two kinds of magnetic fields facilitate the formation of larger droplets. Furthermore, a numerical study (Liu et al. 2011) for axial homogeneous magnetic field-controllable ferrofluid droplet generation clearly showed the inner flow structure throughout the whole formation process. However, the influence of local field and programmable magnetic signal in flow-focusing device on the droplet size and formation mechanism in squeezing regime is still missing.

Here, we present a microfluidic chip-based continuous magnetic droplet generation method for quickly controlling the size of ferrofluid droplets. External local magnetic field generated by magnetic tweezer device was applied perpendicular to the upstream microchannel. We demonstrate that the applied magnetic field leads to a versatile and reliable modulation of droplet size in the squeezing regime of production. Magnetoviscous effect and magnetic drag effect are studied to give a clear understanding of droplet breakup dynamics. Square wave magnetic field can be used to periodically generate droplets with different sizes.

2 Experiment

2.1 Device fabrication

The microfluidic devices were fabricated using standard soft lithography (Duffy et al. 1998). First, a layout editor (CorelDRAW) was used to design the devices. The schematic and dimensions of flow-focusing configurations used in the experiments are shown in Fig. 1a. Next, a master mold was fabricated using the negative SU-8 photoresist (SU-8-2050, MicroChem). The thickness of the mold, which defines the rectangular channel depth, is 100 μm. Polydimethylsiloxane (PDMS) mixture (10 A:1 B) was then poured onto the master mold. After degassing in a vacuum desiccator for 20 min, it was cured in an 80 °C convection oven for 30 min. Then, the cast PDMS was peeled from the SU-8 mold and punched using a manual puncher (Harris Uni-Core, World Precision Instruments). Fluidic access holes with a diameter of 1.2 mm were created. The cast PDMS was then washed in ethanol for 5 min followed by rinsing in distilled water. After the cleaning process, the PDMS parts were then placed in an oven at 80 °C for 10 min to ensure that the surface was free of water. Finally, oxygen plasma treatment (WH-1000, Wenhao) was used to

bond the device. Before use, the chips were left at 65 °C for 24 h to ensure full recovery of the PDMS hydrophobicity.

2.2 Synthesis of superparamagnetic nanoparticles

Superparamagnetic Fe_3O_4 nanoparticles (see example in Fig. S1†) were synthesized by the solvothermal method. Briefly, $FeCl_3{\cdot}6H_2O$ (1.08 g), NaAc (4.0 g) and PAA (100 mg) were dissolved in ethylene glycol (10 mL) and diethylene glycol (30 mL) under magnetic stirring. The obtained homogeneous yellow solution was transferred to a Telfon-lined stainless steel autoclave and sealed to heat at 200 °C. After reaction for 12 h, the autoclave was cooled to room temperature. The obtained magnetic particles were washed with ethanol and water four times, respectively. Then they were dried into a powder under vacuum and dispersed in deionized water with 30 % mass concentration. All magnetic solutions were redispersed under ultrasound for 5 min before use. Figure 1b, c shows the TEM image and magnetization curve of Fe_3O_4 nanoparticles.

2.3 Experimental setup and procedure

The uniform magnetic field was generated using a magnetic tweezer (Rich et al. 2011) with 1500-turn coil assembled around an iron core. A separation gap of 7 mm ensures that the generated magnetic field is homogeneous and uniform. Next, the microfluidic devices were positioned in the middle of the gap (Fig. 1d). The channel of the dispersed phase is aligned perpendicular to the magnetic field. The magnetic flux densities were measured using a commercial gaussmeter (HT20, Cestsen) with an accuracy of ±2 %. A DC power source (selfmade, can be programmed) was used to vary the magnitudes of the magnetic flux density by changing the applied electric current. A high-speed camera (FASTCAM SA5 1000 k-M3, Photron) was used to capture the droplet formation process. Two syringe pumps (LSP02-1B, LongerPump) were used to deliver the fluids through polyethylene (Smiths medical, 0.38 mm ID, 1.09 mm OD) into the microfluidic devices (see example in Figs. S2†, S3†).

Images of the droplet formation process were acquired at a rate of 4000 frames per second. Sizes of ferrofluid droplets were evaluated using customized image processing software ImageJ. The produced ferrofluid droplets are monodispersed with a polydispersity (defined as the standard deviation of the droplet size divided by the average droplet size) of <5 %. The magnetic flux density of the electromagnet can be varied by changing the supply current.

In our experiment, deionized water and water-based ferrofluid were employed as the dispersed phase to form droplets in plant oil phase. At 25 °C, the density of the ferrofluid is 1333 kg/m^3. The density and viscosity of deionized water are 995 kg/m^3 and 0.8 mPa s, respectively. A plant oil (Golden dragon fish) is used as the continuous phase. The density and viscosity of the plant oil are 796 kg/m^3 and 50 mPa s, respectively. The interfacial tension between the ferrofluid and the plant oil is approximately 1.56 mN/m. The interfacial tension between water and the plant oil is approximately 1.22 mN/m.

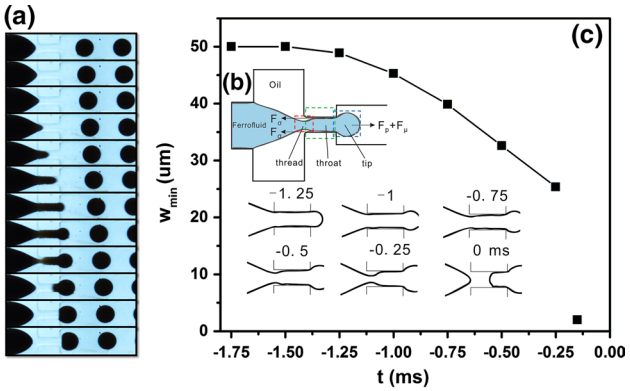

Fig. 2 **a** Formation sequence of ferrofluid droplets in squeezing regime (time interval of each snapshot is 0.5 ms, CP = 1 mL/h, DP = 0.2 mL/h). **b** Various forces the ferrofluid tip suffered in droplet formation progress in the flow-focusing channel. **c** Evolution of minimal width w_{min} of the thread and optical micrographs of the ferrofluid–oil interface along the breakup trajectory (CP = 1 mL/h, DP = 0.2 mL/h)

3 Results and discussion

3.1 Effect of magnetic field on the formation of ferrofluid droplets

In flow-focusing geometry, depending on the properties of immiscible liquids and flow rates of inner and outer phases, droplets occurred in three different modes: squeezing, dripping and jetting (Nie et al. 2008). In the squeezing and dripping regime, the thread of the inner phase broke either in the throat or in the close proximity of the throat. In the jetting regime, a continuous thread of the inner phase extended into the outlet channel and broke far downstream of the throat.

In our experiment, most processes were happened in the squeezing regime and the others were in dripping or higher mode behaviors between squeezing and dripping (secondary droplet phenomenon shown in Fig. 3a). Figure 2a shows the typical preparation of ferrofluid droplet in a squeezing mode. Without applying the magnetic field, ferrofluid and oil start to flow in the chip under the pressure supplied by syringe pumps. Then they meet at the cross-junction and

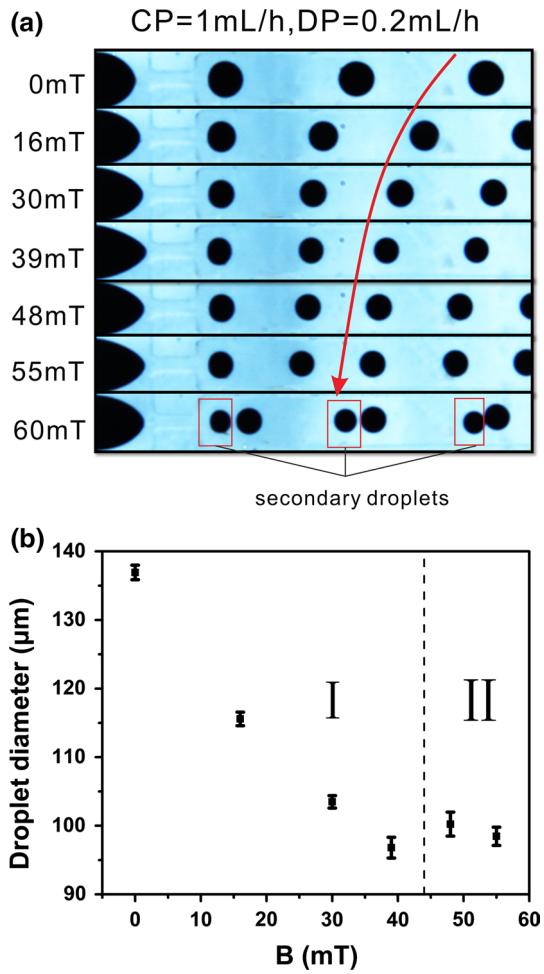

Fig. 3 **a** Ferrofluid droplet micrograph sequences under various magnetic flux densities. The *red arrow* shows the tendency of the droplet size and frequency with the increasing in outer magnetic field. **b** Sizes of ferrofluid droplets as a function of magnetic flux density. The *dash lines* are given for visual guidance

enter the orifice. Oil phase flows through the space around ferrofluid. In this process (Fig. 2b), viscous force F_μ (caused by the viscous stress acting on the interface) and hydrostatic pressure F_p are the main reason leading to the collapse of ferrofluid thread. On the contrary, the interfacial tension force F_σ keeps the ferrofluid tip from moving forward. The balance of the three forces determines the breakup of the droplet. In squeezing regime, because the ferrofluid occupies almost the entire throat, pressure of continuous phase increases dramatically at the region outside ferrofluid thread, and the breakup process can be described by three stages (Garstecki et al. 2005) (Fig. 2c). First, the thread enters the orifice and the width w_{min} of the neck stays constant. Second, a clearly visible neck develops and the thread collapses at a constant rate. In the third stage, the thread collapses rapidly, breaks and retracts upstream of the orifice, and the whole process starts again. In this process, interfacial tension force is larger than viscous force. Capillary number (Ca $= v\mu/\gamma$, where v is the velocity of the continuous phase, μ its viscosity, and γ the interfacial tension) is used to express the relative strength of the two. In squeezing regime, the Ca is low, and the hydrostatic pressure F_p is the key parameter of breakup. In dripping regime, ferrofluid occupies a fraction of space of the throat, continuous phase can flow through the orifice easily without a dramatic change of pressure, and thus F_μ combining with F_σ determines the breakup of droplet. The thread maintains a constant shape, with the pump of inner phase, tip starts to grow, and F_μ stretches the tip moving downstream until the weaker F_σ is no longer strong enough to hold the tip. To this end, the droplet is formed.

To investigate the influence of magnetic flux density, a local magnetic field ($B = 0$, 16, 30, 39, 48, 55, 60 mT) was applied in the upstream of flow-focusing junction. The flow rate was fixed (CP = 1 mL/h, DP = 0.2 mL/h). Figure 3b shows the diameters of the formed ferrofluid droplets in the flow-focusing geometry under different magnetic field B. If B is smaller than 40 mT (Fig. 3b, area I), diameter of droplets decreases with the increasing in B. In comparison with the former works using axial or radial homogeneous global filed (Tan and Nguyen 2011; Wu et al. 2013), local magnetic field played an opposite role in controlling the droplet size. Further increasing the magnetic flux density (Fig. 3b, area II), the average size of droplets stops changing and it almost keeps as a constant around 100 μm. Finally, when B reaches 60 mT, the droplets are no longer monodisperse, and secondary droplets are presented (geometry-determined capillary instability, Shui et al. 2009) (Fig. 3a). Clearly, magnetic field plays an important role in controlling the generation of ferrofluid droplets. The average sizes of the droplets were tunable from 135 to 95 μm by varying the magnetic field from 0 to 60 mT. Moreover, the size of the magnetic droplets can also be tuned by the flow rate, similar to the traditional flow rate controlling method. Therefore, this magnetic controlling method presents bimode controllability. Since magnetic control mode does not rely on the whole flow rate, it would be very important in many applications which need a stable flow rate.

3.2 Formation mechanism for the magnetically controllable droplets

Here, the detailed magnetically controllable mechanism was discussed. As soon as the magnetic field was added on the device, both the magnetoviscous effect and magnetic drag were presented.

Under magnetic field, Fe_3O_4 nanoparticles arranged to form chains-like structure along the direction of magnetic field (see example in Fig. S4†), and the viscosity of ferrofluid was changed. Figure 4 shows this magnetically

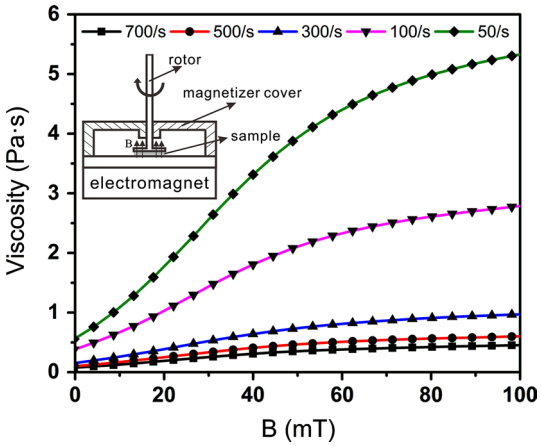

Fig. 4 Rheological test curve of ferrofluid. Viscosity of ferrofluid increases with applied magnetic field at fixed shear rate. The *inset* is the sketch of the Physica MCR301 test system

dependent viscosity of the ferrofluid tested by a commercial rheometer Physica MCR301 (produced by Anton Paar GmbH, Austria) equipped with an electromagnetic accessory MRD180. The sketch of the test system is shown in the inset of Fig. 4. The ferrofluid sample is placed between an electromagnet substratum and an upper rotatable non-magnetism flat rotor. The magnetizer cover is used to strengthen the magnetic field and make it uniform in the area of sample. In general, viscosity of ferrofluid increases with increasing in the magnetic flux density under a fixed shear rate.

To investigate the influence of inner phase viscosity, we compared water and ferrofluid droplets at the same flow condition. Figure 5 illustrates the effect of the value of Q_o/Q_i (flow rate ratio of outer phase and inner phase) on the size of water and ferrofluid droplets, and droplet sequences of this system, respectively. In this experiment, the flow rate of inner phase (Q_i) was kept as a constant (0.2 mL/h). With the increasing in the ratio of the flow rate of immiscible liquids, the droplet diameters decrease (Fig. 5c, area I). The decrease is approximately linear on Q_o/Q_i which means shear mechanism induced strong dependence of droplet diameter and flow rate ratio (Nie et al. 2008). In squeezing regime, the whole formation process of droplets is dominated by hydrostatic pressure F_p and interfacial tension force F_σ. Inner phase blocks the throat, the buildup of F_p in continuous phase squeezes inner phase thread, and a neck evolves through three stages. At the last stage of the collapse induced by F_p, for high-viscosity ferrofluid, the interfacial tension resulted resistance of breakup was stronger than water. As a result, the breakup takes longer time, and the ferrofluid droplets are larger than in the case of low-viscosity water.

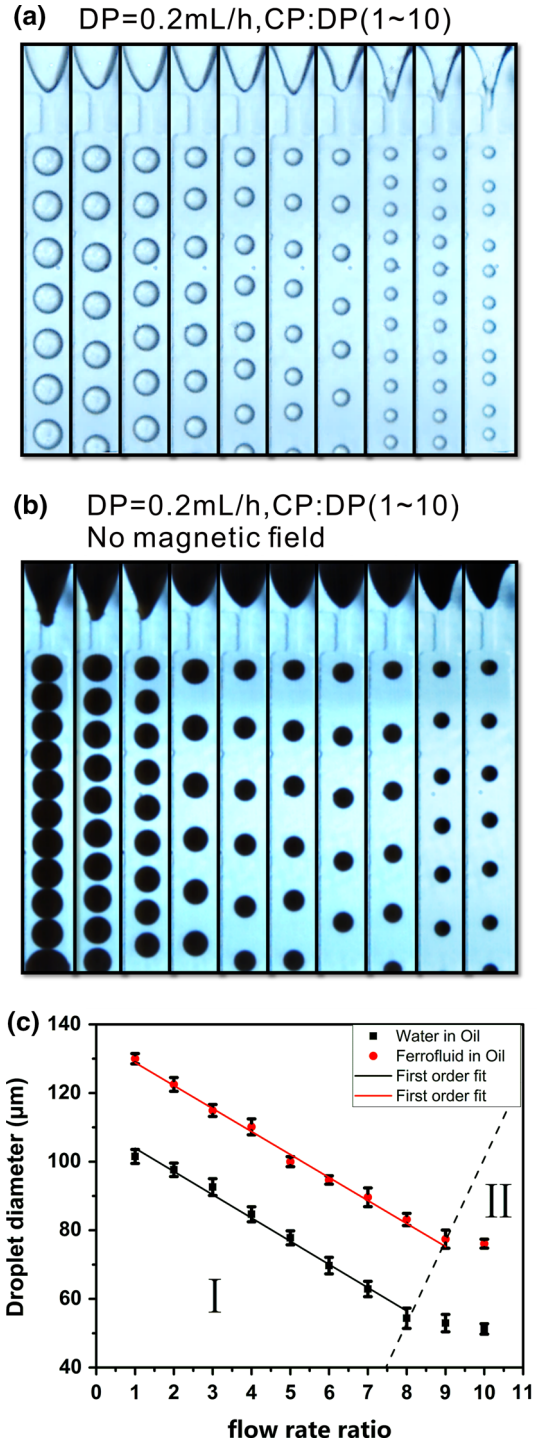

Fig. 5 **a** Water and **b** ferrofluid droplet sequences under various flow rate ratios. **c** Size of water and ferrofluid droplets as a function of flow rate ratio. The *dash lines* are given for visual guidance

As Q_o/Q_i goes on increasing (area II, Fig. 5c), the droplet sizes of both water and ferrofluid decrease slowly, which means the larger the flow rate ratio, the smaller the dependence of droplet size on Q_o/Q_i.

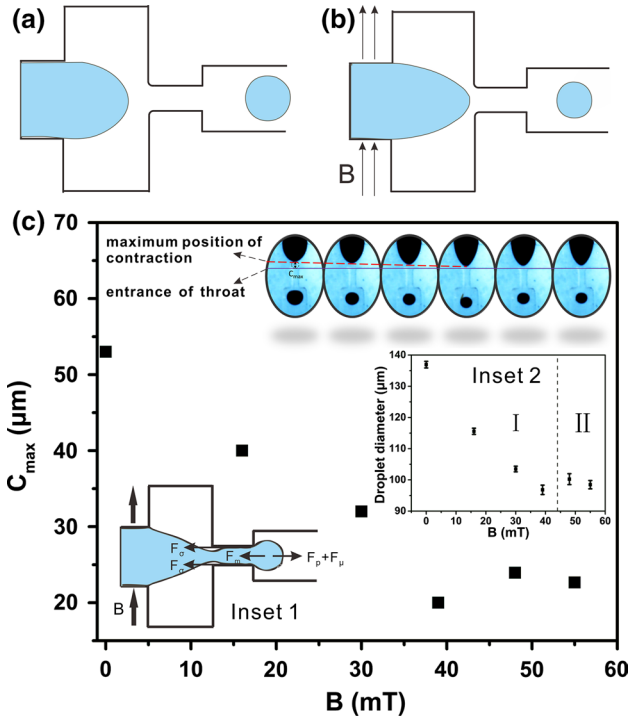

Fig. 6 Maximum contraction position of ferrofluid tip. **a** Illustrations without magnetic field and **b** with magnetic field. **c** Maximum contraction position as a function of magnetic flux density and comparison with droplet size (*inset 2*) and various forces the ferrofluid tip suffered in the droplet formation progress with magnetic field (*inset 1*)

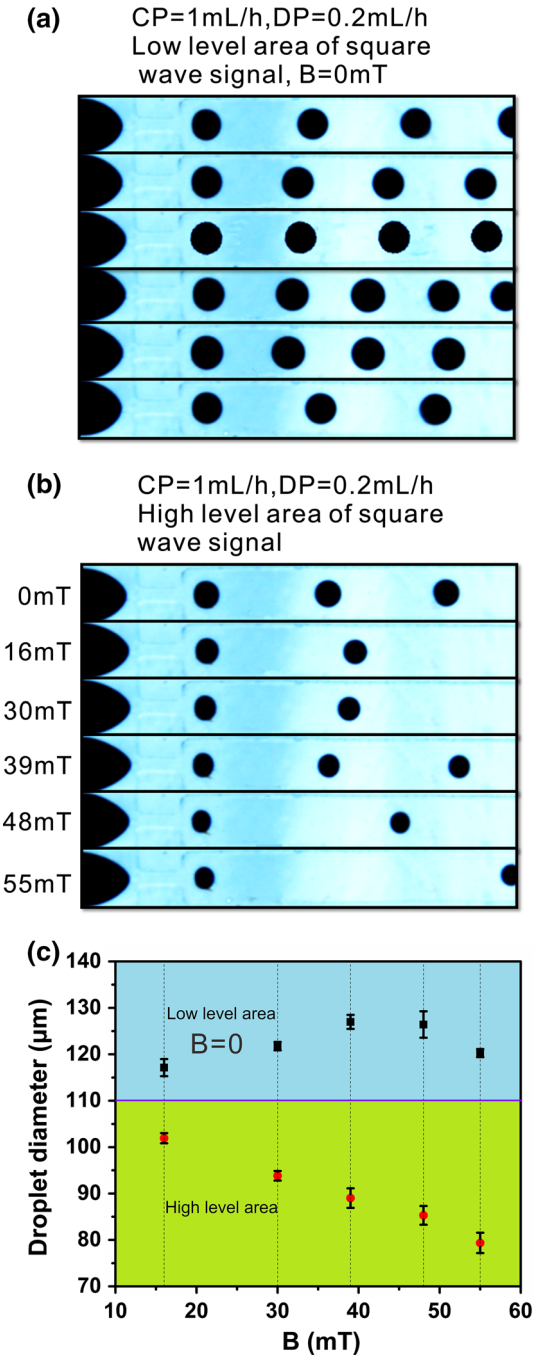

Fig. 7 Droplet formation under square wave magnetic field. **a** Low-level sequences, **b** corresponding high-level sequences, **c** sizes of ferrofluid droplets as a function of magnetic flux density in the two areas of square wave signal

Higher magnetic flux density leads to a higher-viscosity ferrofluid, and higher viscosity of dispersed phase results in an increase in the droplets size (Nie et al. 2008). In contrast to our results, it was found that magnetism plays another role in the formation of ferrofluid droplet.

In squeezing regime, dispersed phase occupies almost the whole throat and continuous phase flows hardly. Thus, the pressure increases dramatically at the region outside ferrofluid thread. Continuous phase starts to squeeze the dispersed phase and a neck induced. Till the neck collapses, droplet breaks up. Continuous phase flows through the orifice freely. When local field is applied on the upstream, the additional magnetic force F_m ($F_m = \mu_0 M \nabla H$, μ_0 is the magnetic permeability of free space, M is the magnetization, and ∇H is the gradient of the external magnetic field strength) (Fig. 6c, inset 1) starts to drag the tip from moving downstream, which leads to a jam at the outlet of the throat. Continuous phase flows through the throat more difficult. Pressure in continuous phase increases faster than the situation without magnetic field. The thinning process of the neck speeds up, which causes the droplet breakup earlier. A relatively smaller droplet is induced. At the moment of droplet breakup, velocity of a new ferrofluid tip and droplet is opposite. A maximum contraction position of ferrofluid tip exists before the next droplet starts to form. Figure 6 shows the maximum contraction position of ferrofluid tip under various magnetic flux densities. Distance between the maximum contraction position of ferrofluid tip and the entrance of throat (C_{max}) firstly decreases with the increasing in magnetic flux density and then nearly keeps constant,

which is similar to the trend of droplet size (Fig. 6c, inset 2). Shorter distance to the entrance of throat leads less time to form the next droplet. Thus, droplet formation frequency increases, and the size decreases.

Magnetoviscous effect results in an increase in droplet size, and magnetic drag effect performs oppositely. It was found that the average size of the droplets decreased with applied magnetic field, which predicted the magnetic drag played a more important role than the magnetoviscous effect. When B reached nearly 60 mT, droplets generated fast enough, the size of the droplets became stable due to the couple effect of magnetic drag and surface tension.

3.3 Controlling the size of the droplet by using square wave magnetic field

Here, the average size of the droplets can be periodically controlled by using square wave signal (Fig. 7). Figure 7c shows the relationship between the diameter and the applied square wave signal. At the high-level area of the signal, droplet size decreases with the increasing magnetic flux density for the reason that magnetic drag force accelerates the droplet breakup. At the same time, magnetic drag force resists the flow of ferrofluid driven by syringe pumps. Inner pressure of ferrofluid grows. When signal goes to the low level, magnetic drag force is disappeared and the pressure decreases between inside and outside of ferrofluid which promotes the flow. The inner phase flows faster than pump actuating speed; thus, bigger droplets are generated. Increasing magnetic flux density leads to an increase in released pressure and thus leads to an increase in droplets size. To this end, magnetic droplets with different size distribution could be periodically obtained by varying the characteristics of the square wave magnetic field.

4 Conclusions

In this work, magnetic field was applied to realize actively controllable generation of ferrofluid droplets in flow-focusing geometry. The average size of the droplets could be simply controlled by varying the intensity of the magnetic field. The breakup dynamics of droplet with magnetic interaction were studied. In comparison with magnetoviscous effect, magnetic drag force played a more important role in the droplet formation process. It was found that maximum contraction distance of the tip was proportional to the droplet size in squeezing regime. Moreover, the square wave magnetic field could be used to periodically generate droplets with different sizes. These results provide new insight into the formation dynamics of ferrofluid droplets under a controlled external force and supply a new way to produce bulk monodisperse droplets with different sizes.

Acknowledgements This work was supported by Collaborative Innovation Center of Suzhou Nano Science and Technology. Financial support from the National Natural Science Foundation of China (Grant No. 11125210), the National Basic Research Program of China (973 Program, Grant No.2012CB937500) and the Anhui Provincial Natural Science Foundation of China (1408085QA17) is gratefully acknowledged.

References

Abdelgawad M, Wheeler AR (2009) The digital revolution: a new paradigm for microfluidics. Adv Mater 21:920–925

Anna SL, Bontoux N, Stone HA (2003) Formation of dispersions using “flow focusing” in microchannels. Appl Phys Lett 82:364

Baroud CN, Delville J-P, Gallaire F, Wunenburger R (2007) Thermocapillary valve for droplet production and sorting. Phys Rev E 75:046302

Diguet A, Guillermic RM, Magome N, Saint-Jalmes A, Chen Y, Yoshikawa K, Baigl D (2009) Photomanipulation of a droplet by the chromocapillary effect. Angew Chem Int Ed Engl 48:9281–9284

Duffy DC, McDonald JC, Schueller OJ, Whitesides GM (1998) Rapid prototyping of microfluidic systems in poly (dimethylsiloxane). Anal Chem 70:4974–4984

El-Ali J, Sorger PK, Jensen KF (2006) Cells on chips. Nature 442:403–411

Fair RB (2007) Digital microfluidics: is a true lab-on-a-chip possible? Microfluid Nanofluid 3:245–281

Garstecki P, Stone HA, Whitesides GM (2005) Mechanism for flow-rate controlled breakup in confined geometries: a route to monodisperse emulsions. Phys Rev Lett 94:164501

Huebner A, Sharma S, Srisa-Art M, Hollfelder F, Edel JB, Demello AJ (2008) Microdroplets: a sea of applications? Lab Chip 8:1244–1254

Jebrail MJ, Bartsch MS, Patel KD (2012) Digital microfluidics: a versatile tool for applications in chemistry, biology and medicine. Lab Chip 12:2452–2463

Jeong WJ, Kim JY, Choo J, Lee EK, Han CS, Beebe DJ, Seong GH, Lee SH (2005) Continuous fabrication of biocatalyst immobilized microparticles using photopolymerization and immiscible liquids in microfluidic systems. Langmuir 21:3738–3741

Link DR, Grasland-Mongrain E, Duri A, Sarrazin F, Cheng Z, Cristobal G, Marquez M, Weitz DA (2006) Electric control of droplets in microfluidic devices. Angew Chem Int Ed 45:2556–2560

Liu J, Yap YF, Nguyen N-T (2011) Numerical study of the formation process of ferrofluid droplets. Phys Fluids (1994–present) 23:072008

Nguyen N-T (2011) Micro-magnetofluidics: interactions between magnetism and fluid flow on the microscale. Microfluid Nanofluid 12:1–16

Nguyen N-T, Ting T-H, Yap Y-F, Wong T-N, Chai JC-K, Ong W-L, Zhou J, Tan S-H, Yobas L (2007) Thermally mediated droplet formation in microchannels. Appl Phys Lett 91:084102

Nie Z, Li W, Seo M, Xu S, Kumacheva E (2006) Janus and ternary particles generated by microfluidic synthesis: design, synthesis, and self-assembly. J Am Chem Soc 128:9408–9412

Nie Z, Seo M, Xu S, Lewis PC, Mok M, Kumacheva E, Whitesides GM, Garstecki P, Stone HA (2008) Emulsification in a microfluidic flow-focusing device: effect of the viscosities of the liquids. Microfluid Nanofluid 5:585–594

Nisisako T, Torii T, Higuchi T (2002) Droplet formation in a microchannel network. Lab Chip 2:24–26

Pipper J, Inoue M, Ng LF, Neuzil P, Zhang Y, Novak L (2007) Catching bird flu in a droplet. Nat Med 13:1259–1263

Priest C, Herminghaus S, Seemann R (2006) Generation of monodisperse gel emulsions in a microfluidic device. Appl Phys Lett 88:024106

Rich JP, Lammerding J, McKinley GH, Doyle PS (2011) Nonlinear microrheology of an aging, yield stress fluid using magnetic tweezers. Soft Matter 7:9933

Ruuge E, Rusetski A (1993) Magnetic fluids as drug carriers: targeted transport of drugs by a magnetic field. J Magn Magn Mater 122:335–339

Schmid L, Franke T (2013) SAW-controlled drop size for flow focusing. Lab Chip 13:1691–1694

Shui L, van den Berg A, Eijkel JCT (2009) Capillary instability, squeezing, and shearing in head-on microfluidic devices. J Appl Phys 106:124305

Song H, Chen DL, Ismagilov RF (2006) Reactions in droplets in microfluidic channels. Angew Chem Int Ed Engl 45:7336–7356

Srinivasan V, Pamula VK, Fair RB (2004) An integrated digital microfluidic lab-on-a-chip for clinical diagnostics on human physiological fluids. Lab Chip 4:310–315

Tan S-H, Nguyen N-T (2011) Generation and manipulation of monodispersed ferrofluid emulsions: the effect of a uniform magnetic field in flow-focusing and T-junction configurations. Phys Rev E 84:036317

Tan Y-C, Cristini V, Lee AP (2006) Monodispersed microfluidic droplet generation by shear focusing microfluidic device. Sens Actuators B 114:350–356

Tan S-H, Nguyen N-T, Yobas L, Kang TG (2010) Formation and manipulation of ferrofluid droplets at a microfluidic T-junction. J Micromech Microeng 20:045004

Teh SY, Lin R, Hung LH, Lee AP (2008) Droplet microfluidics. Lab Chip 8:198–220

Thorsen T, Roberts RW, Arnold FH, Quake SR (2001) Dynamic pattern formation in a vesicle-generating microfluidic device. Phys Rev Lett 86:4163–4166

Velev OD, Prevo BG, Bhatt KH (2003) On-chip manipulation of free droplets. Nature 426:515–516

Woodward A, Cosgrove T, Espidel J, Jenkins P, Shaw N (2007) Monodisperse emulsions from a microfluidic device, characterised by diffusion NMR. Soft Matter 3:627

Wu Y, Fu T, Ma Y, Li HZ (2013) Ferrofluid droplet formation and breakup dynamics in a microfluidic flow-focusing device. Soft Matter 9:9792

Xu J, Li S, Tan J, Wang Y, Luo G (2006) Preparation of highly monodisperse droplet in a T-junction microfluidic device. AlChE J 52:3005–3010

Yobas L, Martens S, Ong WL, Ranganathan N (2006) High-performance flow-focusing geometry for spontaneous generation of monodispersed droplets. Lab Chip 6:1073–1079

Zhang K, Liang Q, Ma S, Mu X, Hu P, Wang Y, Luo G (2009) On-chip manipulation of continuous picoliter-volume superparamagnetic droplets using a magnetic force. Lab Chip 9:2992–2999